

## Substrate-mediated interactions of Pt atoms adsorbed on single-wall carbon nanotubes: Density functional calculations

Hieu Chi Dam,<sup>1,2,3</sup> Nguyen Thanh Cuong,<sup>1</sup> Ayumu Sugiyama,<sup>1</sup> Taisuke Ozaki,<sup>1</sup> Akihiko Fujiwara,<sup>1</sup> Tadaoki Mitani,<sup>1,2</sup> and Susumu Okada<sup>4,5</sup>

<sup>1</sup>Japan Advanced Institute of Science and Technology, 1-1 Asahidai, Nomi, Ishikawa 923-1292, Japan

<sup>2</sup>Japan Science and Technology, ERATO, Shimoda Nano-Liquid Process Project, 2-5-3 Asahidai, Nomi, Ishikawa 923-1211, Japan

<sup>3</sup>Hanoi University of Science, 334 Nguyen Trai, Thanh Xuan, Hanoi, Vietnam

<sup>4</sup>Institute of Physics and Center for Computational Sciences, University of Tsukuba, Tsukuba 305-8571, Japan

<sup>5</sup>CREST, Japan Science and Technology Agency, 4-1-8 Honcho, Kawaguchi, Saitama 332-0012, Japan

(Received 9 January 2009; published 20 March 2009)

In this study, we perform density functional calculations to investigate the interplay between single-wall carbon nanotube (SWNT) supports and adsorbed Pt atoms. We found that adsorption of Pt atoms on SWNTs is found to depend heavily on the curvature of SWNTs. The supporting SWNTs mediate and enhance the range of interactions between Pt adatoms. The long-range interactions originate from the structural deformation of the tube and the complex electronic states formed during the adsorption. Furthermore, these SWNT-mediated interactions significantly modify the diffusion barriers of Pt adatoms on the tube surface.

DOI: [10.1103/PhysRevB.79.115426](https://doi.org/10.1103/PhysRevB.79.115426)

PACS number(s): 61.46.Bc, 61.46.Fg, 71.15.Mb, 73.22.-f

### I. INTRODUCTION

Pt nanoclusters and Pt-alloy nanoclusters on support materials have shown considerable promise in improving catalytic activities and reducing the use of Pt loading in catalysis processes and fuel-cell technology.<sup>1-3</sup> The catalytic activities of Pt-based nanoclusters can be drastically changed by changing their geometric and electronic factors.<sup>4,5</sup> These factors strongly influence each other and are also influenced by the properties of the support materials.<sup>6</sup> Designing unique and superior catalysts for fuel cells requires detailed theoretical and experimental knowledge of the catalytic properties of the nanoclusters adsorbed on support materials. Therefore, the development of atomistic manipulation methods to fabricate nanoclusters of desired sizes and shapes on support materials and the investigation of the catalytic activities of these clusters are extremely important.

One of the most realistic methods to synthesize nanoclusters on support materials is to disperse single atoms on the surfaces of support materials and to manipulate the aggregation and cluster formation of these atoms. Recently, we succeeded in synthesizing highly dispersed size-controlled Pt nanoclusters on a carbon nanotube (CNT) (Ref. 7) from single adatoms. The process by which Pt atoms aggregate on a CNT is considered to be directly related to the process by which adsorbed atoms migrate between adjacent stable adsorption sites. In this migration process, the diffusion barriers and the interactions between adatoms at stable adsorption sites play important roles. However, the dynamic properties of single Pt atoms adsorbed on a CNT are still unclear. In particular, the question regarding the existence of substrate-mediated interactions<sup>8,9</sup> between adsorbates on the surface of low-dimension CNTs, the role of this interaction in the mass transport of adatoms on the substrate,<sup>10</sup> as well as the influence of this interaction on the morphology of the nanoclusters are matters of considerable interest. It is necessary to elucidate the behavior of the Pt atoms adsorbed on CNTs for developing an atomistic manipulation method for the ad-

sorbed nanoclusters and for designing superior heterocatalysts.

In this study, we investigate the interplay between single-wall carbon nanotube (SWNT) supports and adsorbed Pt atoms using the first-principles density functional theory (DFT). We found that adsorption of Pt atoms on SWNTs depends heavily on the curvature and the chirality of SWNTs. The supporting SWNTs mediate and enhance the range of interactions between the Pt adatoms. These long-range interactions were found to originate from the structural deformation of the supporting SWNTs and the complex electronic states formed during the adsorption. Further Pt atoms adsorbed on a SWNT surface can rather easily migrate from site to site, and the diffusion is anisotropic and depends on the tube radius. The substrate-mediated interactions significantly modify the diffusion barriers of Pt adatoms on the tube surface.

### II. CALCULATION DETAILS

All calculations in this study are based on the DFT and performed using the Dmol<sup>3</sup> (Refs. 11 and 12) and OpenMX (Refs. 13–15) codes. We use the generalized gradient functional PBE developed by Perdew *et al.*<sup>16</sup> to evaluate the exchange-correlation energy of interacting electrons. The density functional semicore pseudopotential<sup>17</sup> is chosen to describe the interactions between the valence electrons and the core of Pt. Double-valence plus single-polarization orbitals are used as the basis set. All calculations are performed using *k*-point sampling (0.05 Å<sup>-1</sup> spacing) of the Brillouin zone of periodic supercells. In the present study, we select armchair (*n*, 0) SWNTs, zigzag (*n*, *n*) SWNTs, and graphene sheets as substrates for the adsorption of Pt atoms. The SWNTs are simulated by assuming them to be isolated and infinite in length or extent. The vacuum regions are sufficiently large for the interactions between the SWNTs to be ignored.

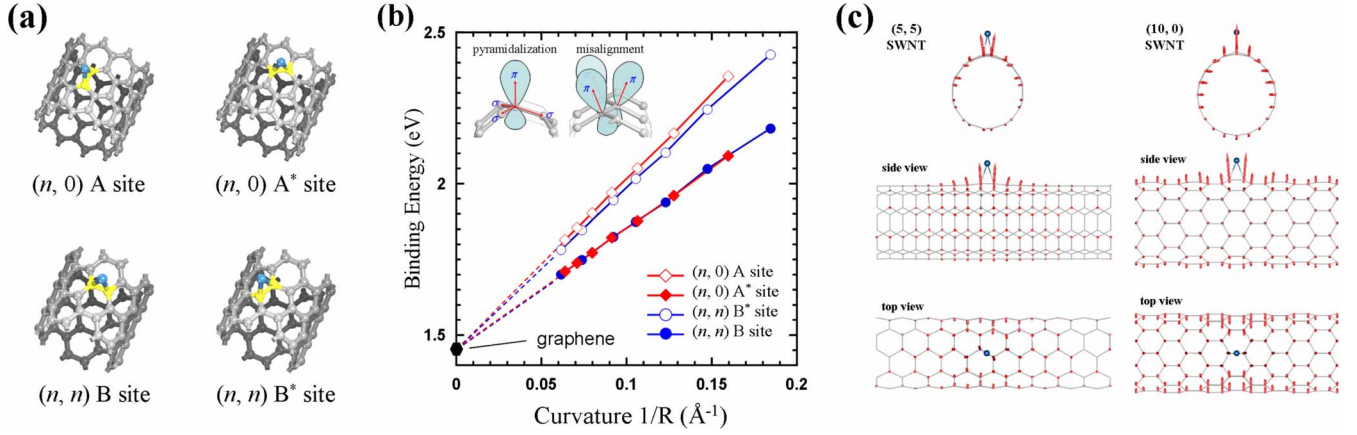


FIG. 1. (Color online) (a) Adsorption configurations of a Pt atom at  $A$  and  $A^*$  bridge sites of  $(10, 0)$  SWNT and at  $B$  and  $B^*$  bridge sites of  $(5, 5)$  SWNT. (b) The curvature dependence of the adsorption energy of single Pt atom on bridge sites of carbon nanotube supports. Open and solid squares are for  $A$  sites and  $A^*$  sites in the  $(n, n)$  carbon nanotubes; open and solid circles are for  $B^*$  sites and  $B$  sites in the  $(n, n)$  carbon nanotubes. Insets show the curvature-induced pyramidalization and misalignments of  $\pi$  orbitals of carbon networks in SWNTs. (c) Displacement of C atoms in  $(5, 5)$  and  $(10, 0)$  SWNTs due to the adsorption of a Pt atom, visualized by gOpenMol (Refs. 25 and 26). The lengths of the arrows are 10 times the actual displacement of the C atoms.

The relaxed structures of Pt atoms adsorbed on the SWNT have been optimized carefully without any constraint. For all optimized structure calculations, all atoms in the system are relaxed until the forces are less than 0.002 hartree/bohr. Binding energy of Pt atoms on the SWNT is computed using the expression

$$E_{\text{bind}} = E_{\text{Pt}} + E_{\text{SWNT}} - E_{\text{Pt/SWNT}}, \quad (1)$$

where  $E_{\text{Pt}}$  represents the total energy of an isolated Pt atom,  $E_{\text{SWNT}}$  represents the total energy of an isolated SWNT, and  $E_{\text{Pt/SWNT}}$  represents the total energy of a SWNT with Pt adatom. For density of states calculations, we use  $1 \times 1 \times 16$   $k$ -points mesh to get the resolution of 0.02 eV Gaussian broadening.

### III. RESULTS AND DISCUSSION

#### A. Structural deformation of SWNTs due to adsorption of Pt atoms

First, the adsorption of the Pt atoms on different sites of the  $(n, n)$  armchair and  $(n, 0)$  zigzag nanotubes are investigated in detail from both geometric and electronic viewpoints. We show the energetically favorable structures of Pt atoms adsorbed on the CNT in Fig. 1(a). The bridge site is found to be the most favorable adsorption site for the adsorption of the Pt atom. Among the C-C bridge sites, the  $A$  and  $B^*$  sites on the  $(n, 0)$  SWNTs and  $(n, n)$  SWNTs, respectively, are the most stable sites for Pt adsorption on the respective SWNTs. Further, our thorough investigation finds that the binding energies between Pt atoms and bridge sites increase linearly with the curvature of SWNTs [Fig. 1(b)] from 2.42 eV [adsorption on  $B^*$  sites of a  $(4, 4)$  SWNT] to 1.45 eV [adsorption on bridge sites of a graphene sheet].

As shown in Fig. 1(c), for both  $(n, n)$  armchair and  $(n, 0)$  zigzag CNTs, the C atoms attached by the Pt atom strongly protrudes from the wall of CNTs and the protrusion behavior of C atoms spreads out to some extent. The strong protrusion

indicates the hybridization between  $d$  states of Pt and  $\pi$  states of CNTs that transforms the  $sp^2$  states of adjacent C atoms to the  $sp^3$ . The shape of the supporting tubes is found to deform from cylindrical to elliptic cylindrical. The curvature-induced *pyramidalization* of carbon networks in SWNTs together with the deformation and the protrusion of the C atoms increases the local curvature of tubes at the adsorption sites, thereby promoting the hybridization between Pt and CNT and increasing the binding energy of the adatoms.<sup>18</sup> The contribution of the hybridization between Pt and CNT, therefore, is considered to be the origin of the linear relation between the binding energy and the curvature of supporting tubes [Fig. 1(b) inset]. In addition, our calculations also show remarkable differences in binding energies of single Pt atoms with  $A$  sites and with  $A^*$  sites and in binding energies of single Pt atoms with  $B$  and  $B^*$  sites, which make different angles with the axes of the tubes. The *misalignment* of  $\pi$  orbital of carbon networks in SWNTs is considered to be the main reason for this feature [Fig. 1(b) inset]. Further, to evaluate the contributions of the deformation of the whole tube and the protrusion of the C atoms, calculations for systems comprising a Pt atom adsorbed on a  $(5, 5)$  SWNT and on  $(10, 0)$  without deformation corroborate that the deformation of the supporting SWNTs increase the adsorption energy by up to 0.8 eV. Thus, the deformation of the supporting SWNTs decreases their strain energy but significantly increases the adsorption energy of the Pt adatoms. A competition in causing a deformation of the supporting SWNT can be expected for a system having several adatoms.

#### B. Interaction between two adsorbed Pt atoms

Next, the issues of interest are the interaction between Pt adatoms and the substrate effect on it, which may provide beneficial information for atomic manipulation of metal clusters on CNT supports.<sup>19</sup> Figure 2(a) shows the binding energy of the Pt atoms adsorbed on the  $(5, 5)$  and  $(10, 0)$  CNTs evaluated by

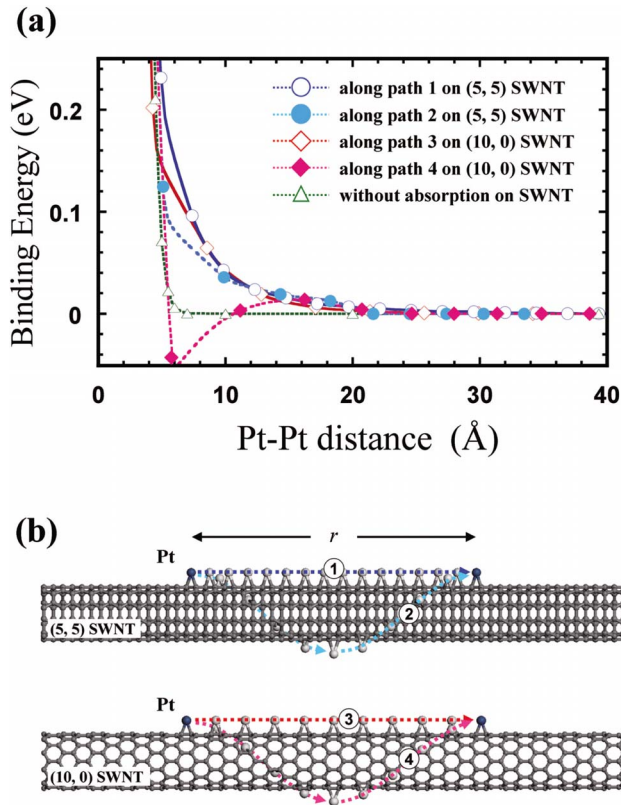


FIG. 2. (Color online) (a) Dependence of binding energy on Pt-Pt distance. Open and solid circles indicate the Pt atoms aligned linearly and helically, respectively, along the axes of the (5, 5) SWNT. Open and solid squares indicate the Pt atoms aligned linearly and helically, respectively, along the axes of the (10, 0) SWNT. Open triangles indicate the nonadsorbed Pt atoms. (b) Structural models of the supercells of SWNTs with Pt adatoms and aligning paths of two Pt atoms used in the calculation.

$$E_{2\text{Pt}/\text{SWNT}}^{\text{bind}}(r) = E_{2\text{Pt}/\text{SWNT}}^{\infty} - E_{2\text{Pt}/\text{SWNT}}^r, \quad (2)$$

where  $E_{2\text{Pt}}^{\infty}$  and  $E_{2\text{Pt}/\text{SWNT}}^r$  are the total energies of the Pt-CNT systems for the Pt atoms are separated by a very large distance (half of the size of the supercells and  $\approx 20$  Å) and by the distance  $r$ . The binding energies of the Pt adatoms are calculated for systems in which one adatom is fixed and the other approached it along four paths on the SWNTs; the unfixed adatom is aligned and approaching the fixed adatom either linearly [paths 1 and 3 in Fig. 2(b)] or helically along the tube axes [paths 2 and 4 in Fig. 2(b)]. The binding energies of the Pt adatoms on a SWNT become significant when their interatomic distance is less than 15 Å. In contrast, for two nonadsorption Pt atoms, we cannot find significant interaction until the interatomic distance becomes less than 7 Å. On the other hand, when the interatomic distance between the Pt adatoms is less than 12 Å, the binding energies depend on the approaching paths. In the region that the interatomic distance is less than 12 Å, the binding energy for the paths 1 and 3 rapidly increases. In contrast, the interactions for the atoms aligned helically along the SWNT axes (paths 2 and 4) are weaker than and can be distinguished from that along the other paths. In particular, the atoms aligned along

path 4 repel each other when their interatomic distance is less than 10 Å. In the region that the interatomic distance is less than 5 Å, the binding energy for all the paths increases rapidly and becomes comparable to that for the nonadsorption atoms.

From the obtained results, we postulate a hypothesis for two principal components of the observed SWNT-mediated interactions between Pt adatoms. The first principal component is the elastic interaction that originated from the deformation of the SWNTs caused by the adsorption of these Pt adatoms. A system comprising more than two adatoms on a SWNT would be less stable when a conflict in the effort to deform the supporting SWNT occurs, giving rise to repulsive interactions between the adatoms. Practically, the elastic interactions between atoms aligned linearly along the SWNT axes (paths 1 and 3) would be caused by the geometrical protrusion of the C atoms in and around the adsorption bridge sites; for adatoms aligned helically along the SWNT axes (paths 2 and 4), the interaction would be caused by both the geometrical protrusion of the C atoms and the deformation from a cylindrical to an elliptic cylindrical shape of the SWNTs. Both kinds of deformation increase the local curvature at the adsorption sites and, therefore, promote the hybridization and binding energy between Pt atoms and the adsorption bridge sites. In fact, we observe no change in the local curvatures of the SWNTs at the adsorption sites for Pt adatoms aligned along paths 1 and 3; however, reductions of up to 2.5% and 4.5% of the local curvatures of the SWNTs are observed for Pt atoms aligned along paths 2 and 4, respectively. The reduction in the local curvatures of the adsorption sites decreases the binding energy of Pt atoms and makes the system become less stable. This can satisfactorily explain the difference in the interactions of the adatoms aligned helically and linearly along the tube axes when the adatoms come close to each other.

The second principal component of the observed SWNT-mediated interactions is the electronic interaction between the complex electronic states formed between the SWNTs and the Pt adatoms. The difference between the charge densities of nanotubes with adsorbed Pt atoms and the sum of the charge densities of an isolated nanotube and of an isolated Pt atom [ $\Delta\rho = (\rho_{\text{Pt}} + \rho_{\text{SWNT}}) - \rho_{\text{Pt on SWNT}}$ ] is calculated in order to evaluate the contribution of the formed complex states to the observed interactions (Fig. 3). It is apparent that the  $d$  electron of the Pt atoms were partially transferred to the nanotubes and distributed over a wide area on the tube surfaces. The different electron density is found to be greater than  $10^{-4}$  a.u. up to a distance of 8 Å from the centers of the adsorption sites. For reference, a simple model comprising two hydrogen atoms<sup>20</sup> is exploited and results to a binding energy in the same order with that of the Pt adatoms when their interatomic distance is greater than 15 Å.

The dependence of the partial density of states (PDOS) of Pt adatoms on their interatomic distance was investigated to clarify the electronic interaction between the complex states formed between the SWNTs and the Pt adatoms. Figure 4 shows the  $d$ -projected PDOS of Pt adatoms aligned along path 1 and two specific molecular orbitals (with  $spd$  hybridized character) of the system with the interatomic distance of 14.76 Å. It is apparent that the PDOS of Pt adatoms shifts



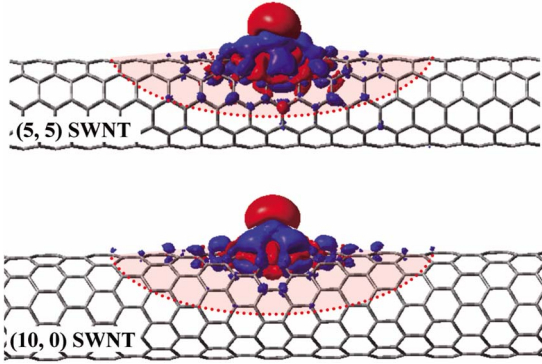


FIG. 3. (Color online) Difference in charge densities of single Pt adatoms on (5, 5) and (10, 0) SWNTs at a  $10^{-4}$  a.u. isosurface value. Red/gray and blue/dark gray colors indicate the positive and negative charged areas, respectively, and the charge flows from the red/gray areas into the blue/dark gray areas.

down when they come closer to each other [Fig. 4(a)]. We confirm substantial hybridization in the electron orbitals of Pt atoms and the metal-adjacent C atoms in the SWNT. Further, we observe bonding states between those hybridized states of the two Pt adatoms [Figs. 4(c) and 4(d)]. When the interatomic distance is less than 8 Å, a direct hybridization in the electron orbitals of the two Pt adatoms can be observed. Consequently, a larger down shift of the PDOS of the Pt adatoms is observed when their interatomic distance decreases from 7.38 to 4.92 Å [Fig. 4(b)]. Similar results are obtained for Pt adatoms aligned along the other paths. These results strongly support our hypothesis and indicate that the complex states were formed due to the adsorption of the Pt atoms and that their penetration inside the SWNTs leads them to bind attractively with each other.

The interactions between the Pt adatoms on a SWNT are analogous to the so-called substrate-mediated interactions, which are well known for various atomic species on metal surfaces.<sup>8,9,21</sup> Note that the one-dimensional tubular structure and the conjugated  $\pi$ -electronic structure of SWNTs are completely different from those of metal surfaces.

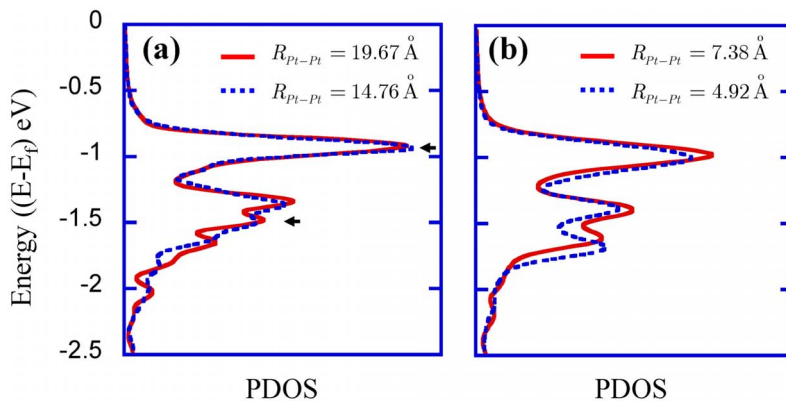


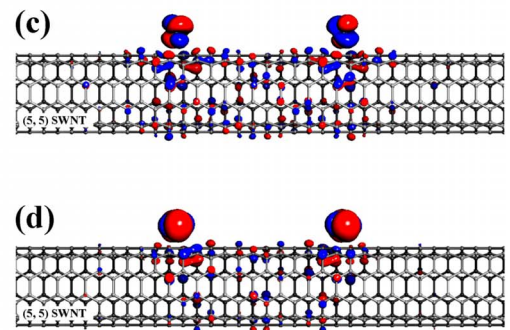
FIG. 4. (Color online)  $d$ -projected PDOS of Pt adatoms aligned along path 1 on the (5, 5) SWNT at different interatomic distances: (a) 19.67 Å and 14.76 Å; (b) 7.38 Å and 4.92 Å. [(c), (d)] The molecular orbitals [at  $E-E_f=-0.93$  eV and at  $E-E_f=-1.48$  eV correspond to the arrows in (a)] of the system in which the interatomic distance is 14.76 Å.

### C. Diffusion of adsorbed Pt atom on SWNT surfaces

Next, the diffusion barriers between adsorption sites<sup>22</sup> for a single Pt adatom are calculated along four pathways linking the bridge sites of the  $(n, 0)$  and  $(n, n)$  SWNTs:  $A$  site  $\leftrightarrow A^*$  site,  $A^*$  site  $\leftrightarrow$  adjacent  $A^*$  site,  $B$  site  $\leftrightarrow B^*$  site, and  $B^*$  site  $\leftrightarrow$  adjacent  $B^*$  site [Fig. 5(a)]. In the case of the diffusion between two adjacent  $A^*$  sites in the  $(n, 0)$  SWNTs, the minimum-energy path passed through the  $A$  site; therefore, though there is an energy barrier between two adjacent  $A^*$  sites, a transition state does not exist. All other cases have transition barriers and the transition points are located near the midpoints of the pathways linking two adsorption sites and are slightly shifted toward the common C atom of the two C-C bridge sites.

Figure 5(b) shows the dependence of the diffusion barriers on the curvature of the supporting SWNTs for both directions of all pathways. The diffusion barriers decrease linearly with the curvature of the tubes. The energy barriers for the diffusions from the  $A$  site to  $A^*$  site and the  $B^*$  site to  $B$  site are found to be higher than those for the diffusions in the inverse directions because the  $A$  and  $B^*$  sites are the most stable sites for adsorption. The diffusion barriers along the  $B^*$  site to adjacent  $B^*$  site in the  $(n, n)$  SWNTs are comparable to those along the  $A^*$  site to  $A$  site and the  $B$  site to  $B^*$  site and are considerably smaller than the adsorption energy of Pt atom on those sites (Fig. 5). In addition, the diffusion barriers on a flat graphene sheet are equal because of the structural symmetry of the layer. The strong dependence of the diffusion barriers of Pt atoms on the radii of the supporting SWNTs is based on the covalent character of the bonding in the system. The hybridization of the  $d$ -electron states of Pt with the  $s$ - and  $p$ -electron states of the C atoms in the C-C bridge sites is enhanced when the supporting SWNTs have large curvatures; thus, the diffusion barrier would be higher for a Pt adatom to change adsorption sites.<sup>18</sup> However, the charge transfer and the ionic character of the bonding in the system allows Pt adatoms to migrate rather easily on the surface of SWNTs with diffusion barriers (less than 0.22 eV) smaller than one-tenth of the binding energy.

Finally, in order to evaluate the influence of the indirect Pt-Pt interaction on the diffusion barrier of the atoms via the



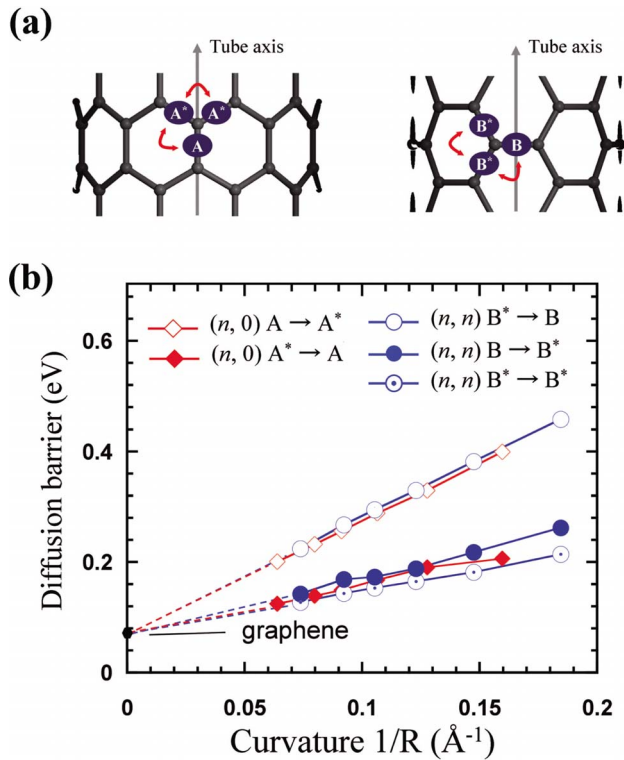


FIG. 5. (Color online) (a) Illustrations of pathways between adsorption sites. (b) Curvature dependence of the diffusion barrier of a Pt atom adsorbed on SWNTs. The open and solid squares indicate the  $A \rightarrow A^*$  and  $A^* \rightarrow A$  pathways, respectively, in the  $(n, 0)$  SWNTs. Open circles, solid circles, and circles with a dot indicate the  $B^* \rightarrow B$ ,  $B \rightarrow B^*$ , and  $B^* \rightarrow B^*$  pathways, respectively, in the  $(n, n)$  SWNTs.

hybrid surface, we calculate the diffusion barriers of the atoms of a system comprising two adsorbed Pt atoms. In both  $(10, 0)$  and  $(5, 5)$  SWNTs, we find that the attractive SWNT-mediated interaction decreases the energy barriers for the diffusion in the direction in which Pt atoms approach to each other and increases the energy barriers for the diffusion in the opposite direction up to 10%. Furthermore, the diffusion barriers of the pathways aligned helically along the tube axes can be significantly modified by the repulsive interaction via the supporting SWNTs for more than 20%.

The obtained results are in good agreement with our experiment,<sup>7</sup> in which the adsorbed Pt atoms tended to aggregate to form clusters on the SWNT surface. Practically, in our experimental study, we found that Pt clusters diffuse and aggregate rather easily on the surface of pristine carbon nanotubes; therefore, introduction of thiol groups on the surface of a carbon nanotube is indispensable in order to obtain highly dispersed Pt nanoparticles. Further, the observed substrate-mediated interaction suggests a significant diffusion barrier for large clusters whose adsorption causes much larger deformation to the supporting CNT. Obstruction to the

aggregation of large clusters is therefore expected and consistent with our experimental observation that the size of the formed nanocluster is determined by the annealing temperature.<sup>7</sup> In addition, the obtained results predict an enlargement in the effective area of interaction of adsorbed Pt clusters due to their formed complex electronic states with the supporting SWNT. It will be interesting to study the substrate-mediated interactions between metal clusters and adsorbed gas molecules on SWNTs, their effect on the dynamic behavior of adsorbed gas molecules on the surface of SWNTs, as well as the catalytic activities of adsorbed metal atoms and clusters.

The observed adsorption and diffusion of Pt atoms, as well as the substrate-mediated interactions between them on SWNTs come from the interplay between  $d$  electrons of transition-metal atoms and  $\pi$  electrons of an aromatic system. This interplay is regarded much in studies of organometallic compounds, which consist of two or more ligands (aromatic molecules) bound to a central metal atom. In organometallic compounds, the ligands can rotate around the central metal atom and the flexibility and number of ligands (coordination number) have an important role in the catalytic reactivity, particularly in the catalytic asymmetric synthesis.<sup>23</sup> On the other hand, in the metal adsorbed on a CNT system, the aromatic network works as a support material with rigid structure. Metal atoms/clusters have flexibility in diffusion and changing adsorption configuration on this supporting aromatic surface. Further, the electron states of metal interact with a much larger  $\pi$ -electron system.

#### IV. CONCLUSION

In summary, we have investigated the interplay between single-wall carbon nanotube supports and adsorbed Pt atoms using the first-principles DFT. We found that adsorption of Pt atoms on SWNTs depend heavily on the curvature and the chirality of SWNTs. The supporting SWNTs mediate long-range interactions between two adatoms that originate from the structural deformation of the SWNTs and the complex electronic states formed during the adsorption. The diffusion barriers of the Pt adatoms are rather small and depend on the radii and the chirality of the supporting SWNTs. Furthermore, we also found that the SWNT-mediated interactions modify the diffusion barriers significantly.

#### ACKNOWLEDGMENTS

This research was partly supported by the Special Coordination Funds for Promoting Science and Technology commissioned by the MEXT, Japan, by the Special project QGTD.08.09 commissioned by the Vietnam National University-Hanoi, and by Toyota Co., Ltd. The computations presented in this study were performed at the Center for Information Science of the Japan Advanced Institute of Science and Technology.

- <sup>1</sup>F. Raimondi, G. G. Scherer, R. Kotz, and A. Wokaun, *Angew. Chem., Int. Ed.* **44**, 2190 (2005).
- <sup>2</sup>R. Bashyam and P. Zelenay, *Nature (London)* **443**, 63 (2006).
- <sup>3</sup>J. Zhang, K. Sasaki, E. Sutter, and R. R. Adzic, *Science* **315**, 220 (2007).
- <sup>4</sup>N. Tian, Z. Y. Zhou, S. G. Sun, Y. Ding, and Z. L. Wang, *Science* **316**, 732 (2007).
- <sup>5</sup>H. Hakkinen, S. Abbet, A. Sanchez, U. Heiz, and U. Landman, *Angew. Chem., Int. Ed.* **42**, 1297 (2003).
- <sup>6</sup>B. Hvolbak, T. V. W. Janssens, B. S. Clausen, H. Falsig, C. H. Christensen, and J. K. Nørskov, *Nanotoday* **2** (4), 14 (2007).
- <sup>7</sup>Y. T. Kim, K. Ohshima, K. Higashimine, T. Uruga, M. Takata, H. Suematsu, and T. Mitani, *Angew. Chem., Int. Ed.* **45**, 407 (2006).
- <sup>8</sup>K. H. Lau and W. Kohn, *Surf. Sci.* **65**, 607 (1977).
- <sup>9</sup>K. H. Lau and W. Kohn, *Surf. Sci.* **75**, 69 (1978).
- <sup>10</sup>H. Bulou and J.-P. Bucher, *Phys. Rev. Lett.* **96**, 076102 (2006).
- <sup>11</sup>B. Delley, *J. Chem. Phys.* **92**, 508 (1990).
- <sup>12</sup>B. Delley, *J. Chem. Phys.* **113**, 7756 (2000).
- <sup>13</sup>T. Ozaki, *Phys. Rev. B* **67**, 155108 (2003).
- <sup>14</sup>T. Ozaki and H. Kino, *Phys. Rev. B* **69**, 195113 (2004).
- <sup>15</sup>T. Ozaki and H. Kino, *Phys. Rev. B* **72**, 045121 (2005).
- <sup>16</sup>J. P. Perdew, K. Burke, and M. Ernzerhof, *Phys. Rev. Lett.* **77**, 3865 (1996).
- <sup>17</sup>B. Delley, *Phys. Rev. B* **66**, 155125 (2002).
- <sup>18</sup>D. H. Chi, N. T. Cuong, N. A. Tuan, Y. T. Kim, H. T. Bao, T. Mitani, T. Ozaki, and H. Nagao, *Chem. Phys. Lett.* **432**, 213 (2006).
- <sup>19</sup>The large-scale DFT calculations were carried out using the OpenMX code and using the supercells of 32 conventional unit cells of the (5, 5) SWNT and 16 conventional unit cells of the (10, 0) SWNT. All calculations were performed at the  $\Gamma$  point. Structural optimizations without constraint were carried out for each Pt-Pt distance.
- <sup>20</sup>The electron density at a distance of  $r_0=2.135 \text{ \AA}$  far from the nuclear of a hydrogen atom is  $10^{-4}$  a.u. The binding energy of two hydrogen atoms is in order of 10 meV when their interatomic distance is  $2r_0$ .
- <sup>21</sup>K. H. Lau, *Solid State Commun.* **28**, 757 (1978).
- <sup>22</sup>The diffusion barriers of Pt adatoms on SWNTs and graphene sheets were investigated by using the linear synchronous transit (LST) and the quadratic synchronous transit (QST) methods, which are incorporated in the Dmol<sup>3</sup> code developed by Accelrys Software Inc., (Ref. 24) for searching the transition states.
- <sup>23</sup>S. J. Malcolmson, S. J. Meek, E. S. Sattely, and R. R. S. A. H. Hoveyda, *Nature (London)* **456**, 933 (2008).
- <sup>24</sup>T. A. Halgren and W. N. Lipscomb, *Chem. Phys. Lett.* **49**, 225 (1977).
- <sup>25</sup>L. Laaksonen, *J. Mol. Graphics* **10**, 33 (1992).
- <sup>26</sup>D. L. Bergman, L. Laaksonen, and A. Laaksonen, *J. Mol. Graphics Modell.* **15**, 301 (1997).